Supporting Information

Peptide-Controlled Assembly of Macroscopic Calcium Oxalate Nanosheets

*Hao Lu,[1 *] Arne Schäfer,[1] Helmut Lutz,[1] Steven J. Roeters,[3] Ingo Lieberwirth,[1]*

Rafael Muñoz-Espí,[2] Matthew A. Hood,[1] Mischa Bonn,[1] Tobias Weidner[1,3]

[1] *Max Planck Institute for Polymer Research, Ackermannweg 10, 55128, Germany*

E-mail: lu@mpip-mainz.mpg.de

[2] *Institute of Materials Science (ICMUV), Universitat de València, C/ Catedràtic José Beltrán 2, 46980 Paterna, Spain*

[3] *Department of Chemistry, Aarhus University, Langelandsgade 140, 8000 Aarhus C, Denmark*

Table of Content:

1. Peptide Synthesis and Purification

Microwave-Controlled Solid-Phase Peptide Synthesis and Peptide Purification.

LE10 oligopeptides were prepared on a CEM Liberty peptide synthesizer. DMF and NMP were used as solvents and the standard CEM Liberty coupling protocols were followed. To achieve 1 mmol of oligomer, preloaded Wang resins containing glutamic acid were used. The amino acid coupling was facilitated by use of Oxyma Pure/HBTU (0.5 M in DMF) and DIPEA (2 M in NMP).

Deprotection and release of the oligopeptides from the Wang resins was accomplished by 24 h treatment with a cleavage solution containing 95% TFA, 2.5% TIS (as a scavenger), and 2.5% H_2O. The products were filtered and then precipitated in cold diethyl ether and centrifuged before lyophilization. The chemical purity of the oligopeptides was characterized by HPLC.

2. Sample Preparation

0.35mg oligopeptides were dissolved into 1mL MilliQ (D_2O for SFG measurement in amide I region), and injected into the subphase contained in the trough, where the solutions are mixed with 18mL MilliQ, 0.19mL KCl (3M/L, final concentration 28.5mM/L), and 0.78mL KOH (0.1M/L, final concentration3.9 mM/L). The pH of the final solution is 10.87, ensuring the full deprotonation of the acidic residues of glutamic acid. The solution was stabilized in a Teflon trough for 3 hours to allow for peptide adsorption and assembly at the air-water interface. The subphase peptide solution was diluted by a factor of 8 using salt solution (milliQ-KCl-KOH).

1.56 mL $CaCl_2$ (0.1M/L) was injected into the sub-phase of the solution, allowing the Calcium ions to be coordinated with the deprotonated glutamic acid residues of LE10 peptides; after 2 hours peptide−Ca^{2+} ion interaction, the CaC_2O_4 mineralization was initiated by injecting 1.56 mL (0.1m/L) $Na_2C_2O_4$ into the sub-phase of solution. After 20 minutes, the fabricated peptide-CaC_2O_4 films were lifted off using Langmuir-Schaefer technique by either (50 nm) Au coated silicon wafers or (2000 meshes) copper transmission electron microscopy (TEM) grids without supporting carbon film.

The CaC_2O_4 mineralized peptide films on Au were characterized by X-ray diffraction (XRD) and X-ray photoelectron spectroscopy (XPS); the films on the TEM grids were examined by scanning electron microscopy (SEM) and TEM.

3. XPS

XPS was conducted using a Kratos Axis Ultra^{DLD} spectrometer (Kratos, Manchester, England) using an Al Kα excitation source with a photon energy of 1487 eV. The data was acquired in the hybrid mode using a 0° take-off angle, defined as the angle between the surface normal and the axis of the analyzer

lens. Detailed and high resolution XP spectra were collected with setting analyzer pass energy at 80 eV and 20 eV, respectively. Neutralizer was always used during spectra collection. Binding energy scales were calibrated to Au $4f_{7/2}$ emission at 84 eV.[1] A linear background was subtracted for all peak quantifications. The peak areas were normalized by the manufacturer supplied sensitivity factors and surface concentrations were calculated using CasaXPS software. The thickness of LE10 peptide film after 20 minutes mineralization (d_{sample}) was calculated by evaluating the intensity ratios of the C 1s and Au 4f emissions,[2] according to a standard expression:

$$\frac{\frac{Ic}{IAu}(sample)}{\frac{Ic}{IAu}(refer)} = \frac{1-exp\frac{-dsample}{\lambda C1s}}{exp\frac{-dsample}{\lambda Au4f}} \times \frac{exp\frac{-drefer}{\lambda Au4f}}{1-exp\frac{-drefer}{\lambda C1s}} \quad (1)$$

and using hexadecanethiol (HDT) self-assembled monolayer (SAM) with a well-known thickness (d_{refer}) of 19.4 Å as a reference.[3] This value agrees well with the theoretical estimate of the SAM thickness on the basis of the alkyl chain length (1.26 Å per CH_2 moiety),[4] molecular inclination (30−33.5°),[5-6] and Au−S distance (1.8 Å).[7] In equation (1), the attenuation lengths of the C 1s (λ_{C1s}) and Au 4f (λ_{Au4f}) photoelectrons were taken at 28 and 30.9 Å, respectively, corresponding to the respective kinetic energies of 1197 eV (E_C) and 1398 eV (E_{Au}).[8]

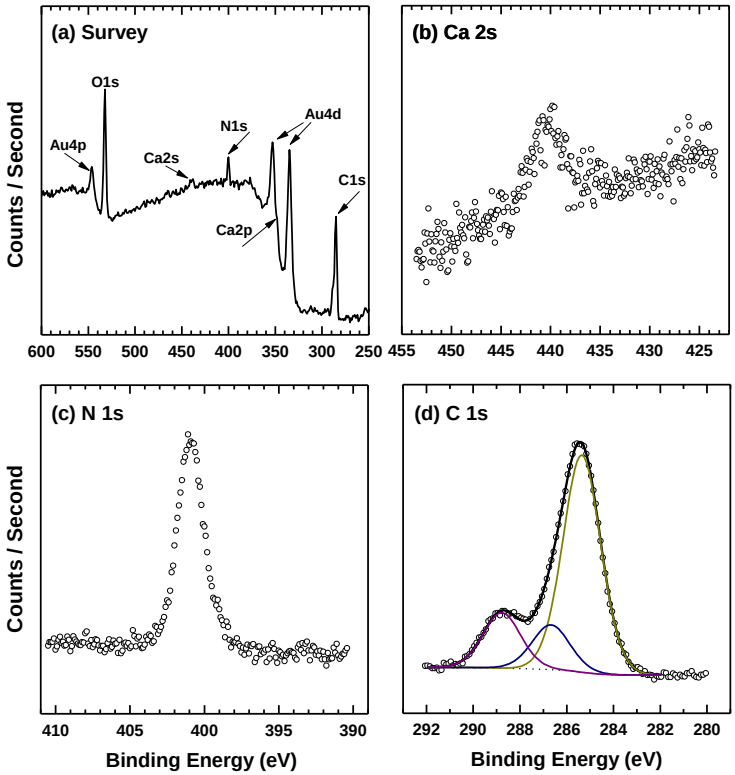

Figure S1. Survey (a), Ca 2s (b), N 1s (c), C 1s (d) XP spectra of LE10 peptides at air-water interface after calcium oxalate mineralization. The C 1s spectra in (d) was self-fitted with individual peaks assigned for the carbon atoms from leucine side chains (dark yellow), peptide backbone (navy), and glutamic acid side chains and oxalate mineral (purple).

Table S1. Summary of XPS determined elemental composition[a] of the CaC_2O_4 mineralized LE10 peptide films at air-water interface.

	O	C	N	Ca	complexed Ca^{2+} per peptide[b]	complexed Ca^{2+} per glutamic acid side chain[c]
LE10-CaC_2O_4	27.2 (0.5)	62.9 (0.3)	8.1 (0.2)	1.86 (0.04)	**~4.4**	**~0.5**
LE10 (theoretical)	24.5	63.8	11.7			

[a] Values in atomic % with experimental errors in parentheses.
[b] complexed Ca^{2+} number per peptide is derived from Ca/N atomic composition ratio by multiplying 19 (Nitrogen atoms in LE10 peptide).
[c] complexed Ca^{2+} number per glutamic acid sidechain is derived from Ca/N atomic composition ratio by multiplying 10 (number of glutamic acid side chain in LE10 peptide)

4. SEM and TEM

SEM measurement was carried out on a Zeiss 1530 LEO Gemini microscope. TEM was carried out with JEM 1400, JEOL Ltd., Japan, and operating voltage of 120 kV was applied during measurement.

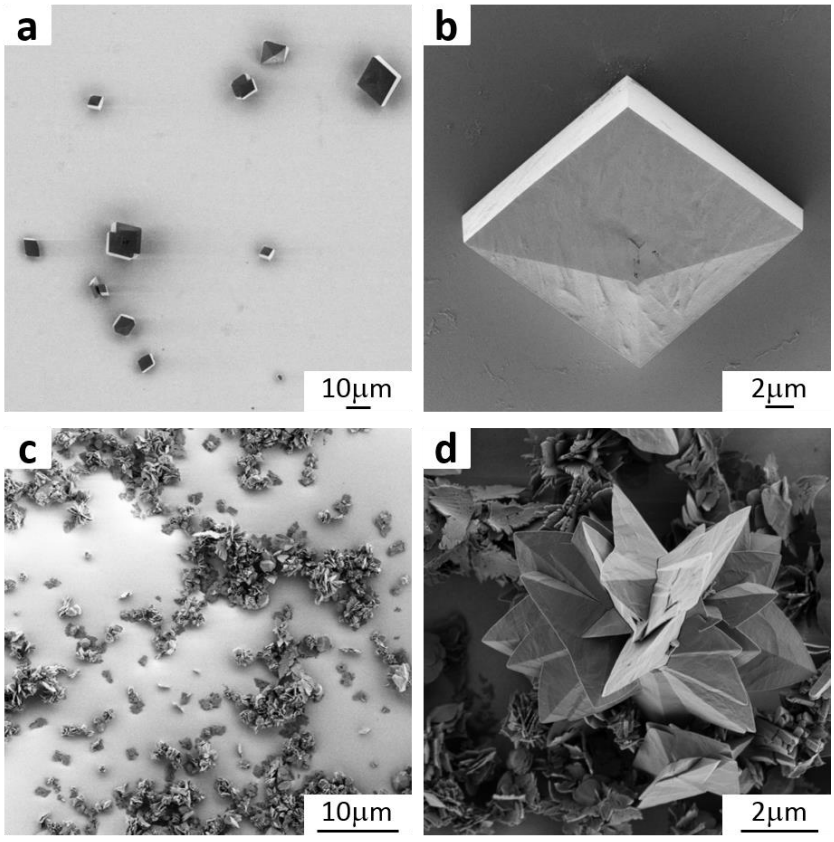

Figure S2. (a-b) SEM images of the calcium oxalate dihydrate polymorph in tetragonal shape mineralized by LE10 peptides at air−water interface. (c-d) SEM images of flake like calcium oxalate monohydrate polymorph mineralized in the absence of LE10 peptides.

TEM examination was done using a FEI Tecnai F20 operated at an acceleration voltage of 200 kV. Micrographs were recorded on a Gatan Ultrascan CCD Camera.

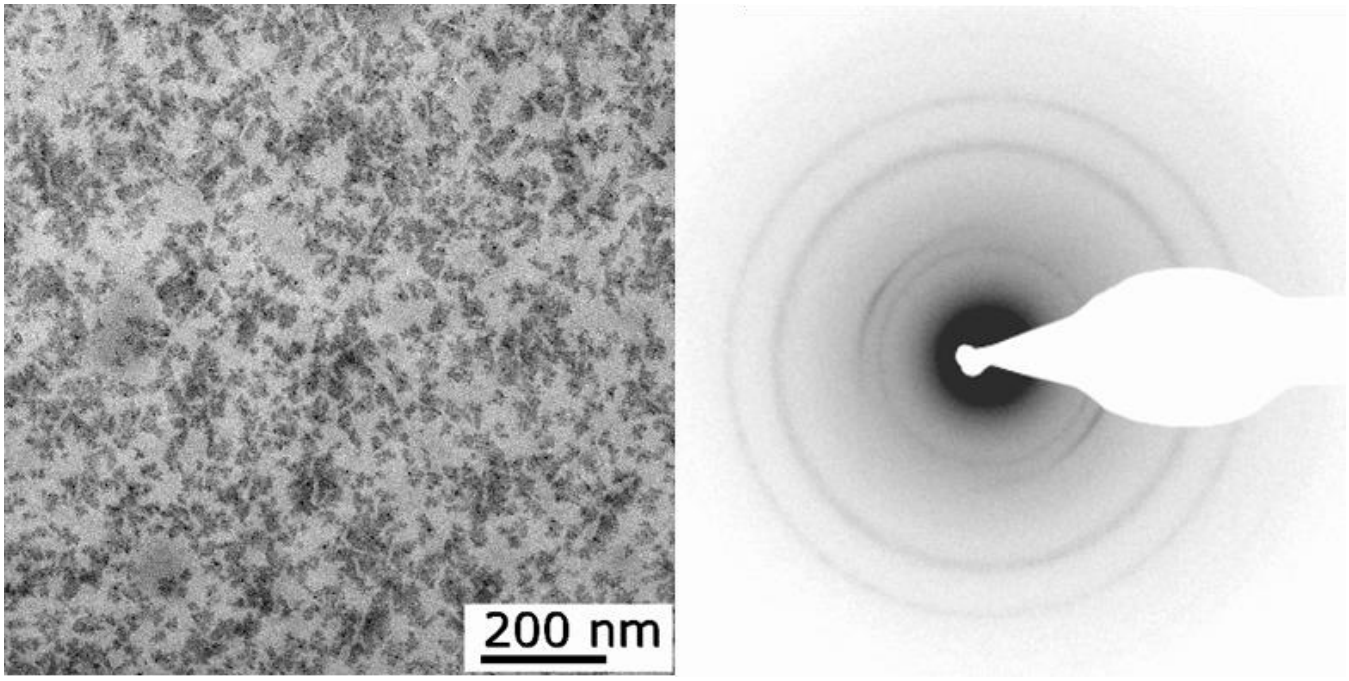

Figure S3. TEM micrograph and the corresponding electron diffraction (ED) pattern from a selected area of the CaC_2O_4 sheet in Figure 1. The ED clearly shows diffuse rings, which refer to lattice distances of 5.3, 4.5, 2.7 and 1.8 Å, respectively. These lattice values do not match well with crystal lattice of calcium oxalate dihydrate, however, the diffuse appearance of the diffraction rings suggest that the oxalate crystals in the sheet are arranged into ordered nuclei in short range.

5. XRD

XRD patterns were recorded on a Phillips PW 1820 diffractometer with an X-ray source producing a Cu Kα wavelength of 1.5406 Å.

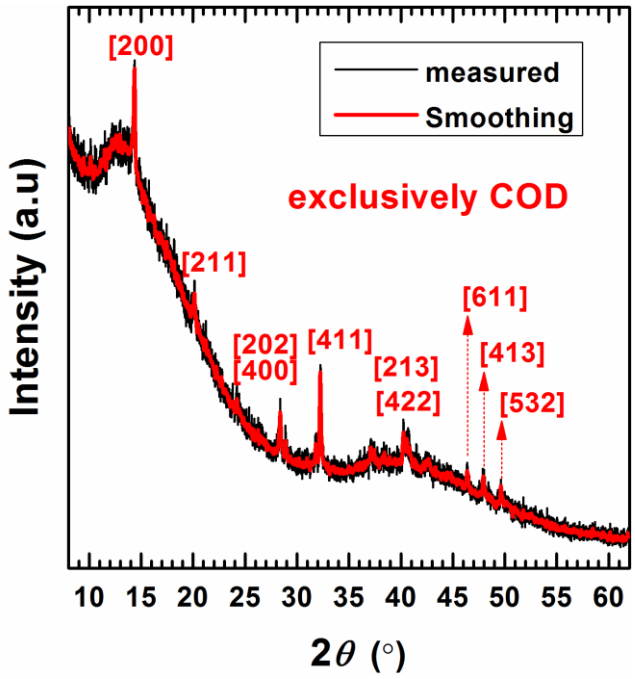

Figure S4. XRD pattern of the calcium oxalate dihydrate mineralized in the presence of LE10 peptides in bulk solution.

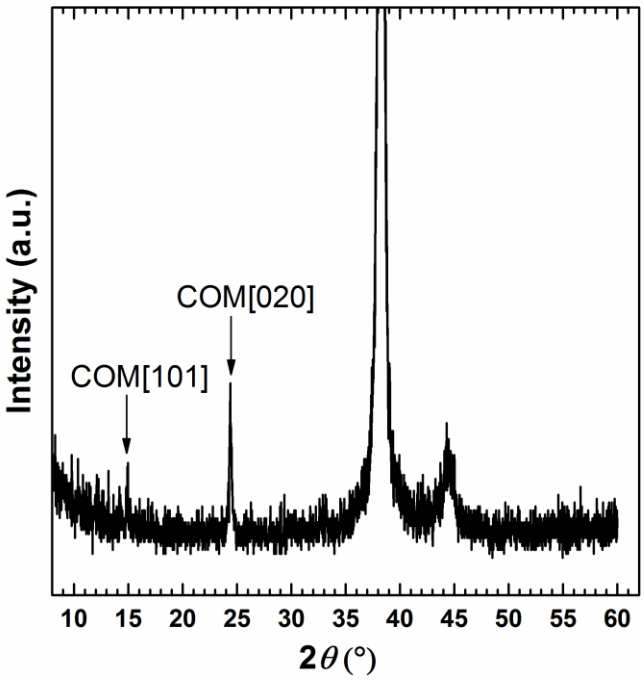

Figure S5. XRD pattern of the calcium oxalate monohydrate mineralized in the absence of LE10 peptides in bulk solution.

6. Vibrational SFG Spectroscopy:

The vibrational SFG spectra were obtained by overlapping in time and space, visible and IR pulses of light. A Ti:Sapphire amplified system (Spitfire Ace, Spectra Physics Inc.) delivers 35 fs long pulses at a central wavelength of ~800 nm and 1 KHz repetition rate. The beam is split in two parts: one it is spectrally narrowed using a Fabry-Perot etalon to achieve spectral resolution (15cm^{-1}, lambda=800, E~25mJ/pulse). The other part is used to generate tunable broadband IR pulses thanks to a parametric optical amplifier followed by a noncollinear difference frequency generation module (TOPAS Prime, LightConversion). The average power at 6000 nm wavelength is 2μJ/pulse. Visible and IR beams are focused onto the sample trough using respectively a 20cm and 5cm focal length lenses. The polarization of both beams can be controlled (s or p) with a polarizer and a half waveplate. Beams are temporally and spatially overlapped at the sample position. The SFG signal is generated with visible and IR beam angles of 55° and 60° respective to the surface normal, and is collimated using a 20cm FL lens, further focused into a spectrograph using a 5cm FL achromatic lens, dispersed by a grating and collected by an intensified CCD camera. The polarization of the SFG signal can also be controlled.

Spectra were recorded in the achiral SPS (sum, visible, and infrared) and chiral PSP polarization combinations. Each spectrum was acquired for 10 minutes, and the spectra are normalized by non-resonance reference spectra of z-cut quartz crystal after background correction, and energy calibration is performed according to the vibration bands of water. D_2O solvents was used due to the spectra interference in amide I region by bending mode of H_2O.

SFG spectra were fitted by Lorentzian peak shapes according to the following equation:[9]

$$I_{SFG} \propto \left|\chi_{eff}{}^{(2)}\right|^2 = \left|\chi_{NR}^{(2)} + \chi_R^{(2)}\right|^2 = \left|A_{NR}e^{i\Phi_{NR}} + \sum_{n=1}^{\infty}\frac{A_n}{\omega_{IR} - \omega_n + i\Gamma_n}\right|^2 \quad (2)$$

In equation (2) : $\chi_{NR}^{(2)}$ and $\chi_R^{(2)}$ are the non-resonant and resonant contributions to the SF signal, respectively. A_{NR} and ϕ_{NR} represent the amplitude and phase of non-resonant term, whereas A_n is the amplitude of *n-th* vibrational mode with resonant frequency ω_n and linewidth Γ_n.

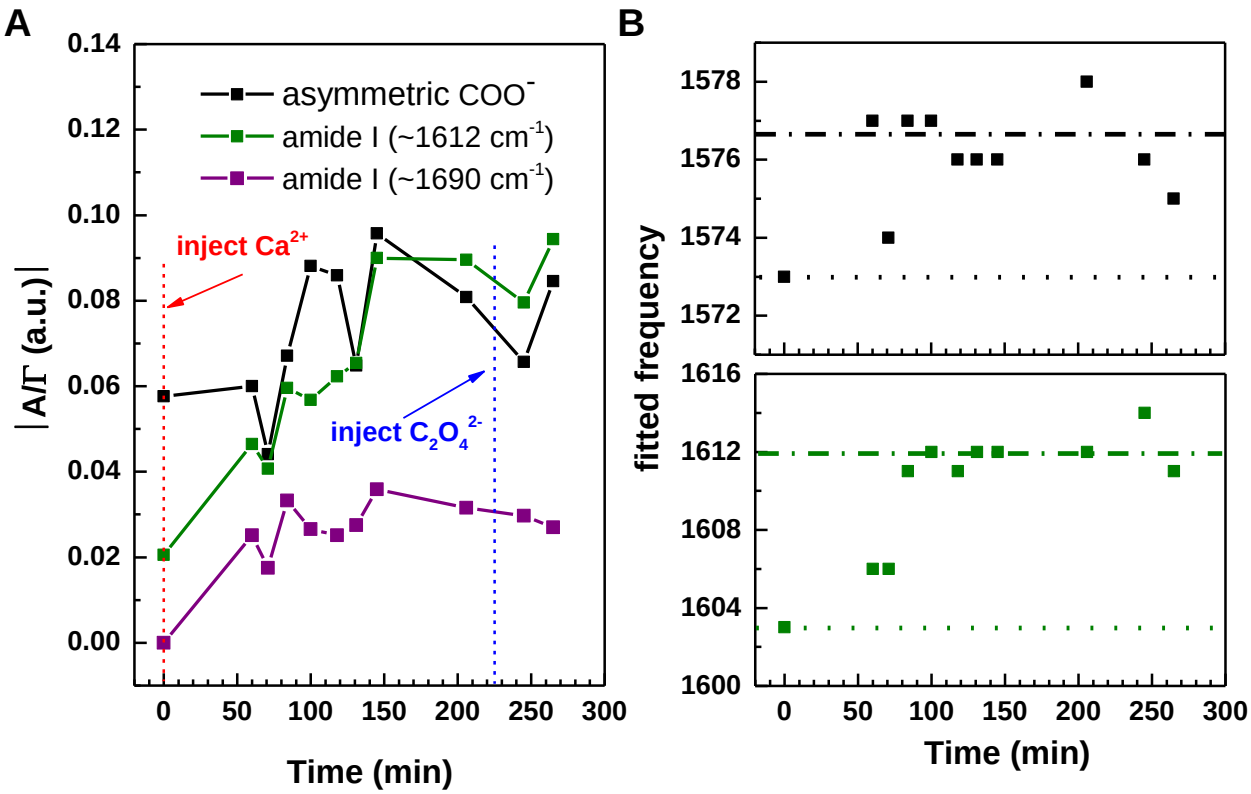

Figure S6. Time dependent A/Γ ratios (A) and frequency ω (B) of the spectra components in Figure 2A for LE10 peptides during Ca^{2+} ion interaction and CaC_2O_4 mineralization. The parameters A, Γ, and ω are derived by fitting SFG spectra according to equation (2).

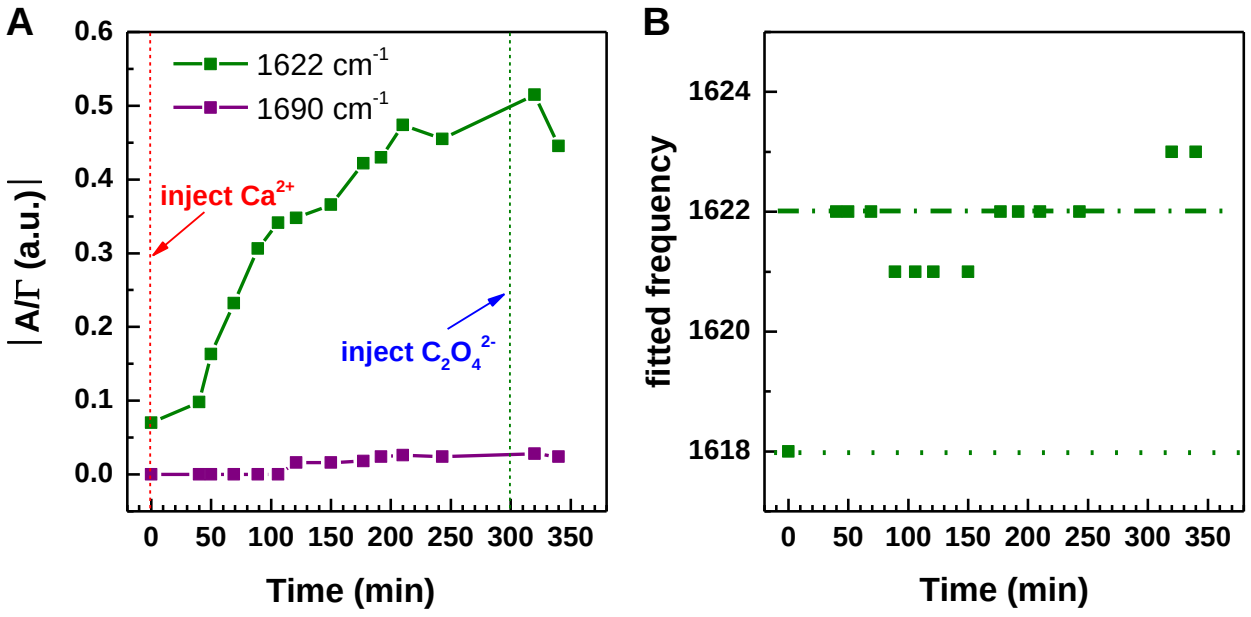

Figure S7. Time dependent A/Γ ratios (A) and frequency ω (B) of the spectra components in Figure 2B for LE10 peptides during Ca^{2+} ion interaction and CaC_2O_4 mineralization. The parameters A, Γ, and ω are derived by fitting SFG spectra according to equation (2).

7. Molecular Dynamics Simulations:

GROMACS 4.6 was used for all simulations.[10] Peptide parameters were taken from the AMBER99SB-ildn force field[11], for calcium the CM parameter set was used.[12] To simulate a water slab, the TIP3P model was used.[13] The simulation box was 9 x 9 x 16 nm in size. Within the box, a 4 nm thick water slab with peptides at the interface was packed with Packmol.[14] The water slab was positioned at half height separating two vacuous spaces of 6 nm in height. Initial configurations of simulation boxes were prepared with twelve beta-sheet LE10 peptides at one of the two vacuum-water interfaces. Simulation boxes were neutralized with an appropriate amount of potassium ions or calcium ions. In order to generate the respective topology and coordinate files, we used the Tleap . The amber input files were subsequently converted to GROMACS input files with Acpype.[15-16] Constraining all bonds using the linear constraint solver (LINCS)allowed for a 2 fs time step. Periodic boundary conditions and the particle mesh Ewald (PME) method was used for electrostatic interactions.[17] Lennard-Jones potential cut-off was set to 1 nm. In order to maintain the temperature at 300 K, velocity rescaling with a stochastic term (v-rescale) was employed.[18] Radial distribution functions were calculated with VMD using in total 890 frames from 445 - 500 ns simulation time.[19] Simulation snapshots were rendered with pymol and VMD.[19]

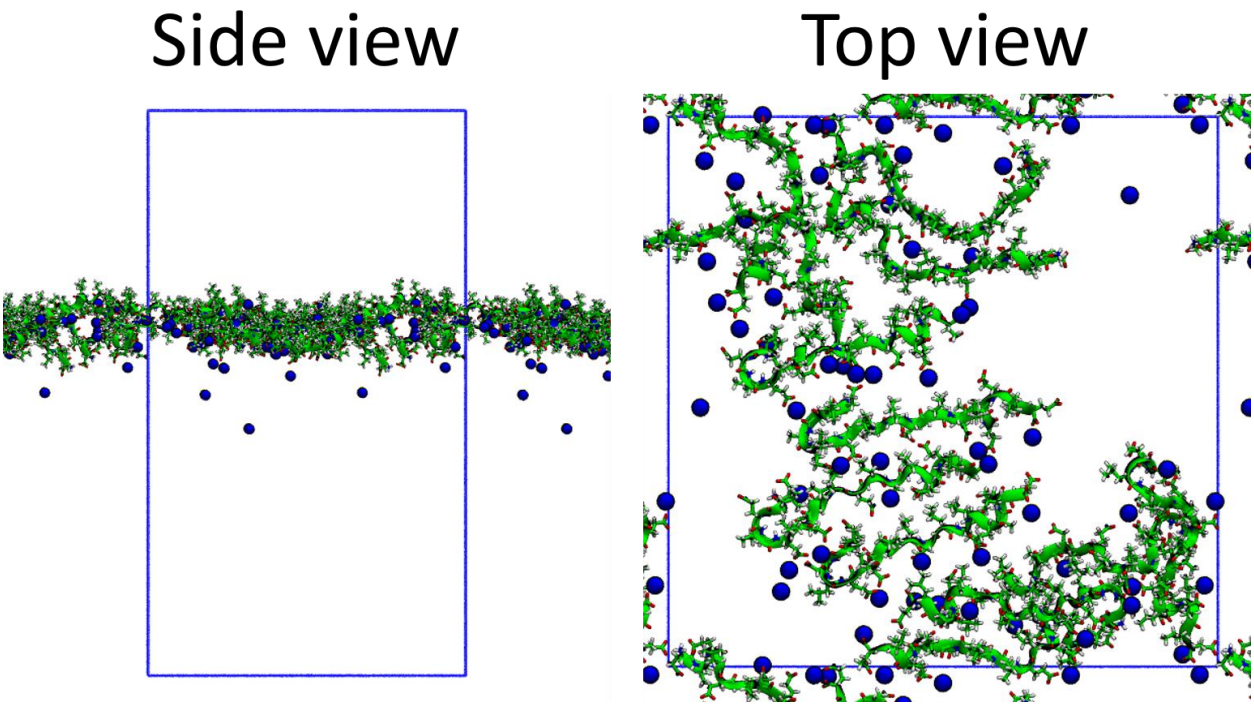

Figure S8. Initial snapshots of MD simulations, Ca ions were randomly placed at the peptide interface in the simulation box. Color scheme: Ca ions blue, peptide backbone green, oxygen red.

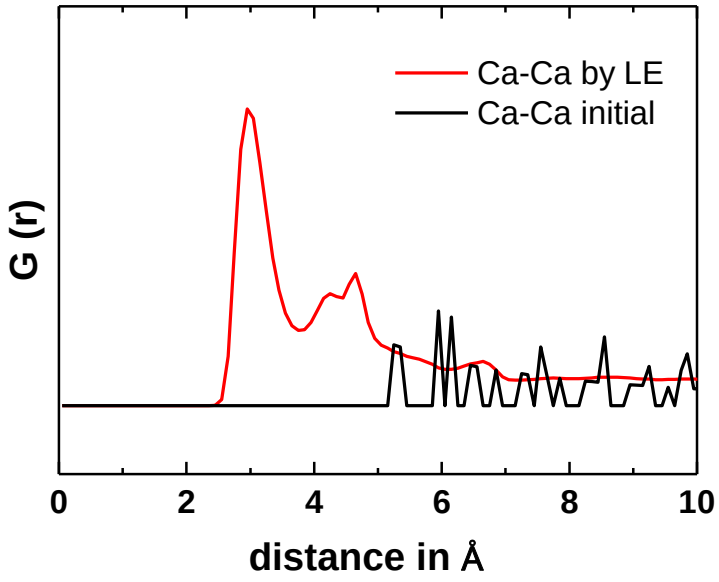

Figure S9. Radial distribution function G(r) of the Ca-Ca distance calculated from the initial and end stage of total simulation time.

8. SFG Spectra Calculation:

The calculated spectra are obtained by constructing one-exciton Hamiltonians for 200 frames (of every 2 ns during the 100 to 500 ns part of the four simulations), according to the formalism described in Ref [20]. Specifically, the couplings between the local amide-I modes are determined from the coordinates of the amide-group atoms, using a parameterized map of an *ab initio* calculation[21-22] for the couplings between neighboring amide groups, which are dominated by through-bond effects, and using the transition charge coupling (TCC) model for the couplings between non-nearest neighbors, as these are dominated by through-space effects.[23] The SFG hyperpolarizabilities of the 200 frames are summed before the response is calculated by taking the absolute square of the total hyperpolarizability. The hydrogenbond-induced local-mode frequency shifts are modelled via the correlation found by Cho *et al.* between the strength of the accepted and/or donated hydrogen-bond(s), the C-O length in the amide groups, and the local-mode amide-I frequency.[24] In practice, we take the C-O length from the coordinates, and apply:

$$n = n_0 + a d r_{CO}$$

with n_0 the base frequency, a the proportionality constant, and $d r_{CO}$ the deviation of the carbon-oxygen bond from its equilibrium value. For the equilibrium value of the carbon-oxygen bond length we used 1.229 Å for amide groups with secondary amines, which corresponds to the equilibrium value of a C-O bond in the AMBER99SB-ILDN force field. For the current study, we

found an optimal match with the experimental spectra for a = 1000. The total linewidth (homogeneous linewidth + FWMH of the visible pulse) was found to be ~16 cm^{-1}, and the base frequency n_0 was 1622 cm^{-1}. To keep the spectral calculations as simple as possible we assumed that there is no non-resonant contribution. This might explain why we find rather large interfacial refractive index (n_i) changes when optimally reproducing the experimental magnitude changes observed upon the addition of Ca^{2+} (see table below).

	LE10	**LE10**+Ca^{2+}
$n_{i,SF}$	4	1
$n_{i,VIS}$	1.3	4.5
$n_{i,IR}$	2	2

9. References:

(1) Moulder, J. F.; Chastain, J.; Sobol, P. E.; Bomben, K. D. *Handbook of X-Ray Photoelectron Spectroscopy*; Perkin-Elmer: Eden Prairie, MN, USA, 1992.

(2) Liu, J. X.; Schupbach, B.; Bashir, A.; Shekhah, O.; Nefedov, A.; Kind, M.; Terfort, A.; Wöll, C. Structural Characterization of Self-Assembled Monolayers of Pyridine-Terminated Thiolates on Gold. *Phys. Chem. Chem. Phys.* **2010**, *12*, 4459–4472.

(3) Biebuyck, H. A.; Bain, C. D.; Whitesides, G. M. Comparison of Organic Monolayers on Polycrystalline Gold Spontaneously Assembled from Solutions Containing Dialkyl Disulfides or Alkanethiols. *Langmuir* **1994**, *10*, 1825–1831.

(4) Walczak, M. M.; Chung, C. K.; Stole, S. M.; Widrig, C. A.; Porter, M. D. Structure and Interfacial Properties of Spontaneously Adsorbed Normal-Alkanethiolate Monolayers on Evaporated Silver Surfaces. *J. Am. Chem. Soc.* **1991**, *113*, 2370–2378.

(5) A., U. *Self-Assembled Monolayers of Thiols*. In *Thin Films*, A., U., Ed. Academic Press: San Diego, CA, 1998.

(6) Ulman, A. Formation and Structure of Self-Assembled Monolayers. *Chem. Rev.* **1996**, *96*, 1533–1554.

(7) Sellers, H.; Ulman, A.; Shnidman, Y.; Eilers, J. E. Structure and Binding of Alkanethiolates on Gold and Silver Surfaces - Implications for Self-Assembled Monolayers. *J. Am. Chem. Soc.* **1993**, *115*, 9389–9401.

(8) Lamont, C. L. A.; Wilkes, J. Attenuation Length of Electrons in Self-Assembled Monolayers of N-Alkanethiols on Gold. *Langmuir* **1999**, *15*, 2037–2042.

(9) Lambert, A. G.; Davies, P. B.; Neivandt, D. J. Implementing the Theory of Sum Frequency Generation Vibrational Spectroscopy: A Tutorial Review. *Appl. Spectrosc. Rev.* **2005**, *40*, 103–145.

(10) Hess, B.; Kutzner, C.; van der Spoel, D.; Lindahl, E. Gromacs 4: Algorithms for Highly Efficient, Load-Balanced, and Scalable Molecular Simulation. *J. Chem. Theory. Comput.* **2008**, *4*, 435–447.

(11) Lindorff-Larsen, K.; Piana, S.; Palmo, K.; Maragakis, P.; Klepeis, J. L.; Dror, R. O.; Shaw, D. E. Improved Side-Chain Torsion Potentials for the Amber Ff99sb Protein Force Field. *Proteins* **2010**, *78*, 1950–1958.

(12) Li, P. F.; Roberts, B. P.; Chakravorty, D. K.; Merz, K. M. Rational Design of Particle Mesh Ewald Compatible Lennard-Jones Parameters for +2 Metal Cations in Explicit Solvent. *J. Chem. Theory. Comput.* **2013**, *9*, 2733–2748.

(13) Jorgensen, W. L.; Chandrasekhar, J.; Madura, J. D.; Impey, R. W.; Klein, M. L. Comparison of Simple Potential Functions for Simulating Liquid Water. *J. Chem. Phys.* **1983**, *79*, 926–935.

(14) Martinez, L.; Andrade, R.; Birgin, E. G.; Martinez, J. M. Packmol: A Package for Building Initial Configurations for Molecular Dynamics Simulations. *J. Comput. Chem.* **2009**, *30*, 2157–2164.

(15) Case, D. A., et al. *Amber 14*; University of California, San Francisco, 2014.

(16) Sousa da Silva, A.; Vranken, W. Acpype - Antechamber Python Parser Interface. *BMC Research Notes* **2012**, *5*, 367.

(17) Darden, T.; York, D.; Pedersen, L. Particle Mesh Ewald - an N.Log(N) Method for Ewald Sums in Large Systems. *J. Chem. Phys.* **1993**, *98*, 10089–10092.

(18) Bussi, G.; Donadio, D.; Parrinello, M. Canonical Sampling through Velocity Rescaling. *J. Chem. Phys.* **2007**, *126*, 014101 (1–7)

(19) Humphrey, W.; Dalke, A.; Schulten, K. Vmd: Visual Molecular Dynamics. *J. Mol. Graph. Model* **1996**, *14*, 33–38.

(20) Roeters, S. J.; van Dijk, C. N.; Torres-Knoop, A.; Backus, E. H. G.; Campen, R. K.; Bonn, M.; Woutersen, S. Determining in Situ Protein Conformation and Orientation from the Amide-I Sum-Frequency Generation Spectrum: Theory and Experiment. *J. Phys. Chem. A* **2013**, *117*, 6311–6322.

(21) Gorbunov, R. D.; Kosov, D. S.; Stock, G. Ab Initio-Based Exciton Model of Amide I Vibrations in Peptides: Definition, Conformational Dependence, and Transferability. *J. Chem. Phys.* **2005**, *122*, 224904 (1–12).

(22) Hamm, P.; Zanni, M. *Concepts and Methods of 2D Infrared Spectroscopy*; Cambridge University Press: Cambridge, 2011.

(23) Hamm, P.; Lim, M. H.; Hochstrasser, R. M. Structure of the Amide I Band of Peptides Measured by Femtosecond Nonlinear-Infrared Spectroscopy. *J. Phys. Chem. B* **1998**, *102*, 6123–6138.

(24) Ham, S.; Kim, J. H.; Lee, H.; Cho, M. H. Correlation between Electronic and Molecular Structure Distortions and Vibrational Properties. II. Amide I Modes of NMA-nD_2O Complexes. *J. Chem. Phys.* **2003**, *118*, 3491–3498.